CARBONATION AND WETTING OF Ca/Si 0.83 AND 1.5 SYNTHETIC C-S-H

Carbonatação e molhagem de C-S-H sintético 0.83 e 1.5 Ca/Si

Monique Palavro Lunardi
University of São Paulo | São Paulo, São Paulo | monique.lunardi@lme.pcc.usp.br

Thiago Ricardo Santos Nobre
University of São Paulo | São Paulo, São Paulo | thiago.nobre@lme.pcc.usp.br

Vanderley Moacyr John
University of São Paulo | São Paulo, São Paulo | vmjohn@usp.br

ABSTRACT

This study explores the carbonation and wetting kinetics of synthetic calcium silicate hydrate (C-S-H) with Ca/Si ratios of 0.83 and 1.5 using in-situ X-ray diffraction (XRD), attenuated total reflection Fourier-transform infrared spectroscopy (ATR-FTIR), and thermogravimetric analysis (TGA). In 0.83 C-S-H, XRD results reveal pure C-S-H phases with no portlandite or $CaCO_3$ polymorphs, corroborating TGA findings. Minor changes suggest water incorporation. Conversely, 1.5 C-S-H exhibits distinct XRD patterns with portlandite peaks, indicating limited $Ca(OH)_2$ reaction. ATR-FTIR spectra confirm carbonation in both, with distinct features. 1.5 C-S-H proved to be more susceptible to carbonation due to enhanced calcium availability. Despite portlandite presence, C-S-H rapidly reacts with CO_2, likely due to its higher surface area. The study offers insights into C-S-H's carbonation behavior and structural changes during CO_2 exposure, valuable for cementitious material applications.

Keywords: C-S-H carbonation, in-situ monitoring, low-calcium C-S-H, high calcium C-S-H.

1 INTRODUCTION

C-S-H (Calcium-Silicate-Hydrate) is the predominant phase in hydrated cement, constituting roughly 75% of its composition (MADDALENA et al., 2019a), varying in cement containing SCM's (LOTHENBACH; SCRIVENER; HOOTON, 2011). It significantly influences the material's strength, porosity, and mass transport properties. Despite decades of study, C-S-H remains not completely understood, especially its transformations during exposure to humidity and carbonation (JOHN; MATSCHEI; STEPHAN, 2018). The structure of C-S-H is frequently described as a defective tobermorite, which has a Ca/Si=0.83, meanwhile, in cement, the Ca/Si varies from 0.7 to 2.1 (LOTHENBACH; NONAT, 2015; TAJUELO RODRIGUEZ et al., 2017).

The Ca/Si ratio controls C-S-H crystal chemistry, pH (10 to 12.4), basal space, crystallite size, mean chain length, bound and interlayer water, and is responsible, in part, for the cohesion of hydrated cement pastes (PELLENQ; VAN DAMME. HENRI, 2004). However, changes in humidity and/or temperature can modify the layer-to-layer distance, and the chemical and mechanical behavior of the system (ROOSZ et al., 2016), which will cause swelling or shrinkage (GAJEWICZ et al., 2016; GAJEWICZ-JAROMIN et al., 2019; SCHULTE HOLTHAUSEN; RAUPACH, 2018; SCRIVENER; JUILLAND; MONTEIRO, 2015).

Carbonation in hydrated cement occurs when carbon dioxide (CO_2) reacts with the calcium-rich phases of cementitious materials, in the presence of water, changing the mineral assemblage and the microstructure. While the existing literature commonly identifies portlandite as the primary reactant with CO_2, (PHUNG et al., 2015) points out that C-S-H may reacts even faster than portlandite, but its kinetics and effect on chemistry and microstructure of various C-S-H composition is not clear. CO_2 is in the atmosphere but also diluted in the mixing water, a concentration that normally depends on the atmospheric pressure of the gas, which varies locally. CO_2 in mixing water allows carbonation without interference with diffusion mechanisms been a predominant dissolution precipitation process (ZAJAC et al., 2023).

The main aim of this paper is to explore the influence of Ca/Si ratio of synthetic C-S-H in its carbonation and water incorporation by in-situ XRD, FTIR and TGA measurements.

2 METHODOLOGY

Two C-S-H samples with Ca/Si ratios target of 0.83 and 1.5 were synthesized via mechanochemical process utilizing a Fritsch Pulverisette 6 classic line planetary ball mill. The reagents employed were pure calcium hydroxide ($Ca(OH)_2$) and amorphous silica commercially available from Sigma Aldrich. Calcium oxide (CaO) was obtained by calcining $Ca(OH)_2$ at 900°C for 4 hours. The reagents were mixed with pure water in a water-to-solid ratio of 4. This mixture was processed in a tungsten jar, undergoing grinding for a total duration of 6 hours, with each cycle consisting of 20 minutes of grinding and 10 minutes of rest, all conducted at 600 rpm. The resulting samples were subsequently dried in a vacuum oven at 40°C.

To perform in-situ XRD carbonation, dried C-S-H samples were mixed with pure water (2g/g) that had been pre-bubbled with CO_2 (resulting in a pH of around 5). After 2 minutes the paste was transferred into a custom-made sample holder produced by a 3D printer and immediately covered with a Kapton polymeric film. The in-situ XRD measurements were conducted using an Empyrean Panalytical diffractometer, operating at 40 kV and 40 mA with CuKα radiation, scanning in the range of 3-45°. A 10-minute scan was recorded every 20 minutes for a total duration of 20 hours, starting immediately after the mixing of dry C-S-H with CO_2-bubbled water.

Figure 1: C-S-H pastes placed in the sample holder with Kapton film



Furthermore, ATR-FTIR analysis was performed using a Shimadzu IRTracer-100 model in the range of 600-4000 cm^{-1}. After the in-situ analysis was completed, the samples were once again dried in a vacuum oven at 40°C. Thermal Gravimetric Analysis (TGA) was made from 25 to 1000°C at a constant heat rate of 10°C/min in an inert N_2 atmosphere. The test was conducted immediately after drying samples to avoid any carbonation during storage.

The mass loss from C-S-H dehydration was calculated between 100°C and 400°C. Since C-S-H lose water in a wide range of temperature and the water content depends on the drying process, literature does not have consensus, varying from 50°C-600°C (SCRIVENER; SNELLINGS; LOTHENBACH, 2016), 105°C-818°C (LI et al., 2020), 25°C-200°C (MADDALENA et al., 2019b), 100°C-350°C (JIN et al., 2022). Equation $\boldsymbol{W_1 = 18.01 X 56.08 + 60.08 + 18.01_X X 100}$ (1 was used to determine stoichiometric formula of the synthetized C-S-H. By TGA results, in 0.83C-S-H the mass loss was 18% and 1.5C-S-H was 20%. Thus, the stochiometric formulas of the synthetized C-S-H are $CSH_{1.3}$ (or $0.83CaO.SiO_2.1.3H_2O$) and $C_{1.5}SH_2$ (or $1.5CaO.SiO_2.2H_2O$).

$$\boldsymbol{W_1 = \frac{18.01_X}{56.08+60.08+18.01_X} X 100} \quad (1)$$

Where, W_1 is the mass loss from C-S-H, 18.01, 56.08 and 60.08 are the molar mass of a Ca/Si =1.

3 RESULTS AND DISCUSSION

Figure 2a and b show the XRD measurements from 0.83 C-S-H over time. The 2θ of around 6.3° (14Å), 14.3°, 29.2° and 32.0° corresponding to C-S-H was found in the 0.83 synthetic C-S-H during the ten first minutes of contact with the CO_2 saturated water. No peak of portlandite or $CaCO_3$ polymorphs was found indicating an extremely pure C-S-H which agrees with the TGA results presented in Figure 2c. Only minor changes were observed during the measurement, primarily marked by an increase in C-S-H and calcite/C-S-H peak at 29°. It's noteworthy that the basal space ratio remained unaltered during the test. The sharpening of the 6.3° peak over time can be attributed to water incorporation and/or preferential orientation of the C-S-H, as variations in relative humidity are known to influence the position and intensity of 001 reflections (GABOREAU et al., 2020). Figure 2c presents the TGA and DTG results of the 0.83 C-S-H. It is worth mentioning that even considering the low availability of calcium in 0.83 Ca/Si ratio, there is an increase in calcite mass after carbonation. The wollastonite (related to the decomposition of C-S-H) peak remained constant. Furthermore, the mass loss prior to carbonation was much higher than after carbonation and the stoichiometric mass loss due to carbonation,

indicating that carbonation makes it difficult for water to leave the sample. The same tendency is not observed in 1.5C-S-H.

Figure 2: a) In-situ XRD patterns from 10 to 1080 minutes for sample Ca/Si=0.83; b) zoom in the 3° to 10° and 28° to 34° range with baseline correction from 10 minutes and 20h carbonation (the background was subtracted for normalization); c) TGA and DTG results of 0.83 C-S-H measured on the dry state.

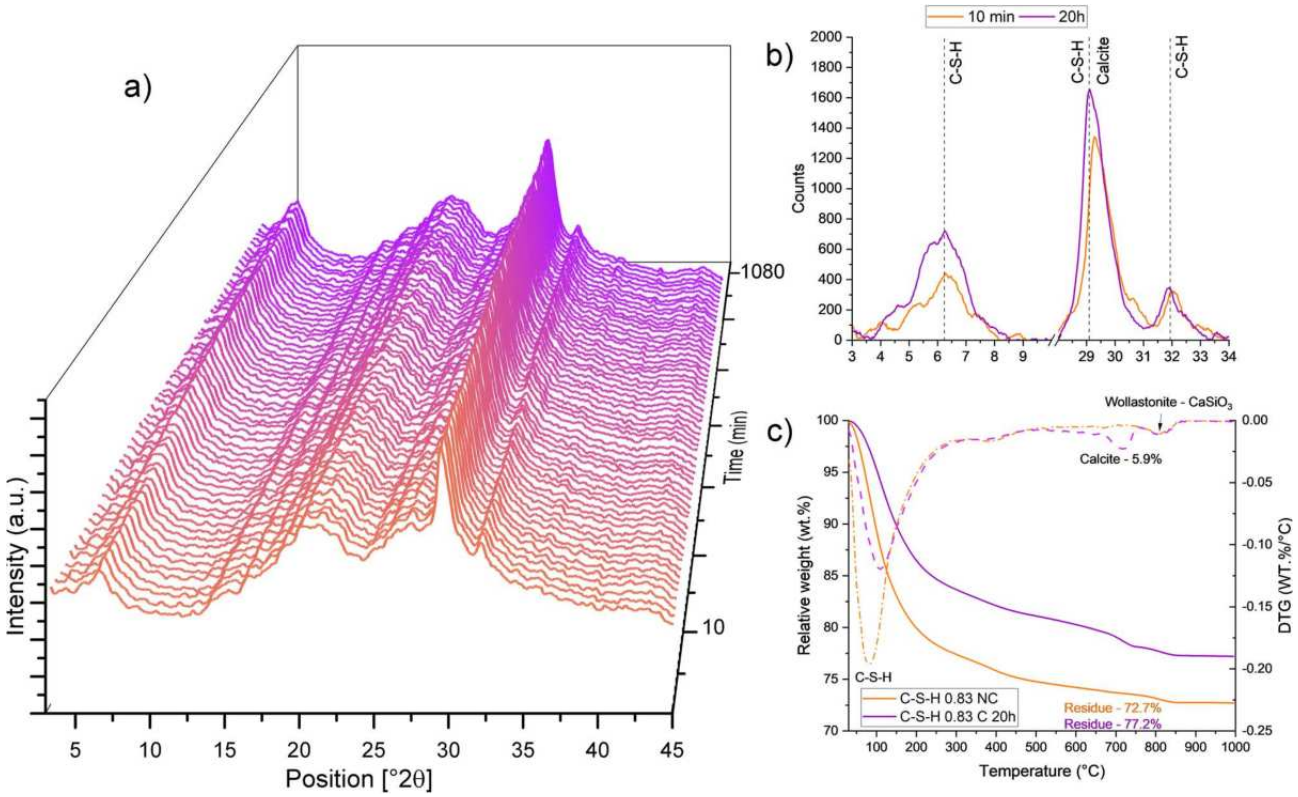

Figure 3 illustrates the XRD pattern of C-S-H 1.5 over-time, which is remarkable different than the one with C/S 0.83. The 2θ of around 6.3° (14Å), 14.1°, 28.01° (anorthic afwillite crystalline-c-s-h) 29.1° and 31.4° corresponding to C-S-H and related crystals was found in 1.5 synthetized C-S-H.

Figure 3: a) In-situ XRD patterns from 10 to 1080 minutes experiment (sample Ca/Si=1.5); b) zoom in the 27° to 35° range with baseline correction from 10 minutes and 20h carbonation (the background was subtracted for normalization); c) TGA and DTG results of 1.5 C-S-H measured on the dry state.

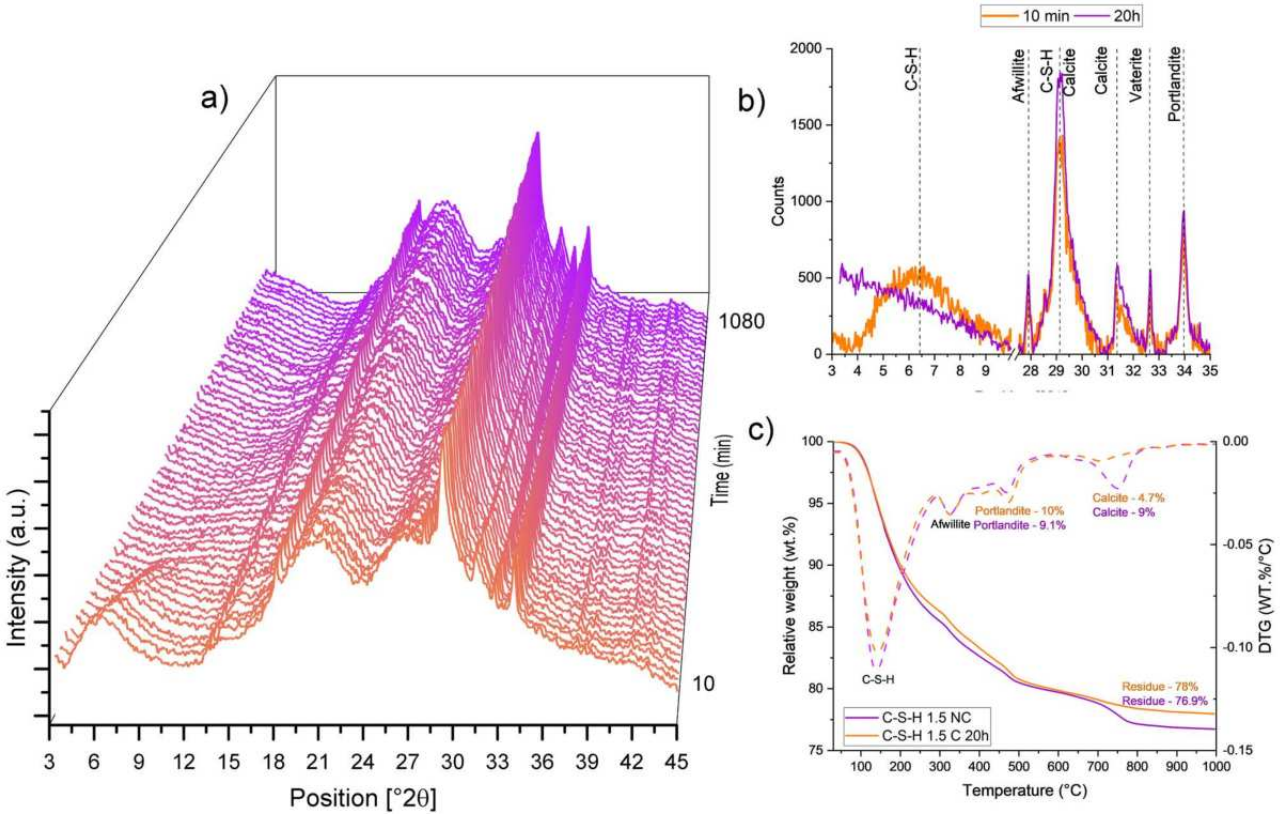

Additionally, portlandite peaks were evident at 18.03° and 34.09°, a found supported by TGA results (Figure 3c**Erro! Fonte de referência não encontrada.**). A vaterite peak presented in 32.7° and calcite in 31.4° indicate a previous carbonation also detected by the TGA measurements. just 4 hours after mixing with water saturated with CO_2, the peaks around 6.3° (C-S-H) and 14.1°(C-S-H) began to diminish, which can be caused due to carbonation and progressive amorphization of the C-S-H structure. Importantly, the crystalline peaks of afwillite and portlandite remained stable throughout the 20-hour carbonation process. These results agreed with the TGA measurements in Figure 3c, as afwillite mass loss does not change, and portlandite loses only 0.9% of the mass. However, peaks corresponding to calcite and vaterite (as shown in Figure 3b) became more pronounced and well-defined after 20 hours of carbonation, suggesting carbonation of the C-S-H. Given the potential overlap between the 29° peaks of C-S-H and calcite, the growth of $CaCO_3$ polymorphs was confirmed through FTIR spectra and TGA measurements. Since TGA shows a growth of 4.3% of calcite, and only 0.9% of portlandite was consumed, this implies that the CO_2 has reacted with the calcium from the C-S-H. This is certainly facilitated by the higher specific surface area of C-S-H compared to portlandite (REGNAULT; LAGNEAU; SCHNEIDER, 2009).

Figure 4 presents the infrared spectra of the two analyzed C-S-H before and after carbonation. Before carbonation, characteristic peaks at 968 cm^{-1} (in 0.83 C-S-H) and the 945cm^{-1} (in 1.5 C-S-H) corresponding to Si-O stretching vibrations of Q^2 was found. The differences in the position of the main peak between 0.83 and 1.5 Ca/Si ratios is attributed to the presence of dimeric silicates (945 cm^{-1}), more popular in high Ca/Si and oligomeric silicates (968 cm^{-1}), primarily found in low-calcium C-S-H (JOHN; MATSCHEI; STEPHAN, 2018).

In the 0.83 C-S-H phase, a broad peak in the 1500-1400 cm^{-1} range and a sharp peak at 875 cm^{-1} (emerging after 20 hours of carbonation) were indicative of $CaCO_3$ polymorphs (also seen in TGA results). Following carbonation, a visible peak appeared at 1100 cm^{-1}, related to silica gel formation, consistent C-S-H decomposition by carbonation. Additionally, a peak at 663 cm^{-1} was observed, associated with Si-O-Si vibrations.

In the case of 1.5 C-S-H, the primary Q^2 peak initially appeared at 945 cm^{-1} and subsequently shifted to 962 cm^{-1} after carbonation, suggesting a decalcification of C-S-H, as also noted by (ZAJAC et al., 2020b). Q_1 bands at 1007 cm^{-1} and 794-805 cm^{-1}, unique to 1.5 C-S-H due to its higher calcium content, are also clearly visible. Following carbonation, a broad band in the 1600-1350 cm^{-1} range, attributed to $CaCO_3$ polymorphs, became evident. Since no aragonite peaks were not observed in XRD measurements, this band probably is from calcite and vaterite. the sharpened peak at 873 cm^{-1} became more pronounced after carbonation and was associated with calcite and.

In both 0.83 and 1.5 C-S-H the main peak related to Q^2 decreased its intensity after carbonation due to C-S-H decomposition.

Figure 4: ATR-FTIR spectra of synthetic C-S-H (0.83 and 1.5) at 10 min an 20h of exposure to water saturated with CO_2

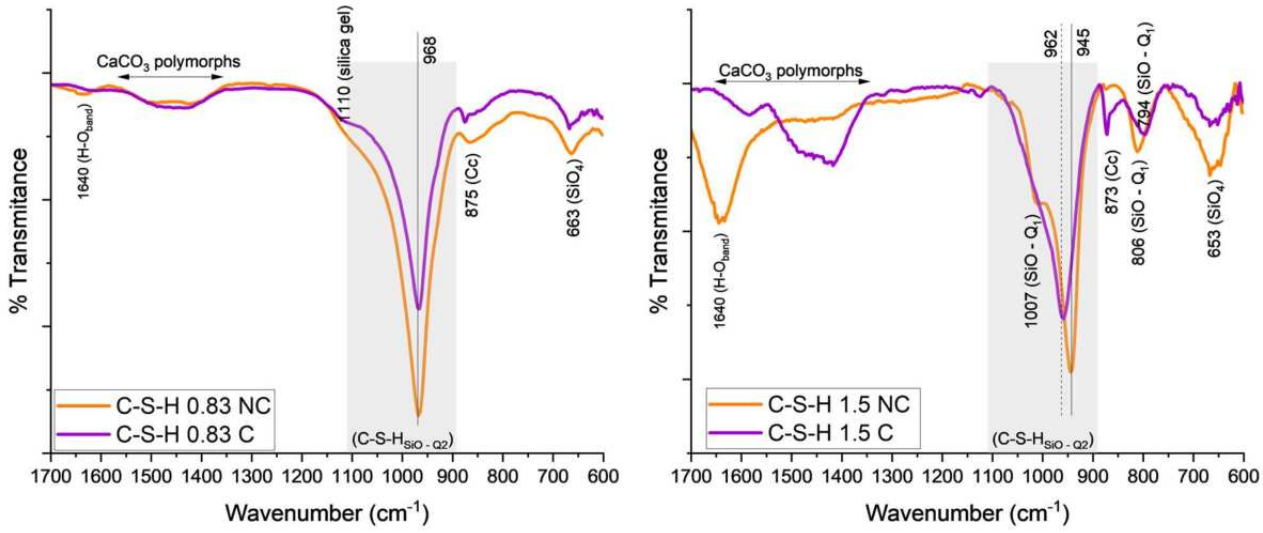

4 CONCLUSIONS

In this work, the transformation overtime of .83 and 1.5 synthetic C-S-H when mixed with CO_2 saturated water was explored by X-ray diffraction, ATR infrared spectroscopy and thermogravimetric analysis. Based on the results the following conclusions can be made:

- Mixing with CO_2 saturated water cause changes in C-S-H microstructure over-time. The effect depends on the Ca/Si ratio.
- Despite portlandite availability in 1.5 C-S-H the CO_2 reaction with C-S-H is more rapidly, probably because its high surface area.
- Carbonation acidifies 1.5 C-S-H changing its 945cm^{-1} band to 962cm^{-1}, similar to 0.83C-S-H main band.
- The methods used in this work proved to be effective for monitoring the development of carbonation and wetting in C-S-H during the first 20h.

These findings contribute to our understanding of the carbonation and wetting behavior of C-S-H and offer insights into its reactivity, crystal formation, and structural changes, which are critical aspects in the context of cementitious materials and their interactions with CO_2.

5 ACKNOWLEDGEMENTS

The author's wish to thanks Portal 3D and Hubic for the sample holder development. This work was supported by CNPq.

BIBLIOGRAPHY

GABOREAU, S. et al. Hydration Properties and Interlayer Organization in Synthetic C-S-H. **Langmuir**, v. 36, n. 32, p. 9449–9464, 18 ago. 2020.

GAJEWICZ, A. M. et al. A 1H NMR relaxometry investigation of gel-pore drying shrinkage in cement pastes. **Cement and Concrete Research**, v. 86, p. 12–19, 1 ago. 2016.

GAJEWICZ-JAROMIN, A. M. et al. Influence of curing temperature on cement paste microstructure measured by 1H NMR relaxometry. **Cement and Concrete Research**, v. 122, p. 147–156, 1 ago. 2019.

JIN, M. et al. Degradation of C–S–H(I) at different decalcification degrees. **Journal of Materials Science**, v. 57, n. 41, p. 19260–19279, 1 nov. 2022.

JOHN, E.; MATSCHEI, T.; STEPHAN, D. **Nucleation seeding with calcium silicate hydrate – A review**. **Cement and Concrete Research**Elsevier Ltd, , 1 nov. 2018.

LI, Y. et al. Carbonation of the synthetic calcium silicate hydrate (C-S-H) under different concentrations of CO2: Chemical phases analysis and kinetics. **Journal of CO2 Utilization**, v. 35, p. 303–313, 1 jan. 2020.

LOTHENBACH, B.; NONAT, A. **Calcium silicate hydrates: Solid and liquid phase composition**. **Cement and Concrete Research**Elsevier Ltd, , 1 dez. 2015.

LOTHENBACH, B.; SCRIVENER, K.; HOOTON, R. D. Supplementary cementitious materials. **Cement and Concrete Research**, v. 41, n. 12, p. 1244–1256, 2011.

LU, B. et al. Characteristics of CSH under carbonation and its effects on the hydration and microstructure of cement paste. **Construction and Building Materials**, v. 364, 18 jan. 2023.

MADDALENA, R. et al. Direct synthesis of a solid calcium-silicate-hydrate (C-S-H). **Construction and Building Materials**, v. 223, p. 554–565, 30 out. 2019a.

MADDALENA, R. et al. Direct synthesis of a solid calcium-silicate-hydrate (C-S-H). **Construction and Building Materials**, v. 223, p. 554–565, 30 out. 2019b.

PELLENQ, R. J. M.; VAN DAMME. HENRI. Why Does Concrete Set?: The Nature of Cohesion Forces in Hardened Cement-Based Materials. **MRS Bulletin**, v. 29, p. 319–323, 2004.

PHUNG, Q. T. et al. Effect of limestone fillers on microstructure and permeability due to carbonation of cement pastes under controlled CO2 pressure conditions. **Construction and Building Materials**, v. 82, p. 376–390, 2015.

REGNAULT, O.; LAGNEAU, V.; SCHNEIDER, H. Experimental measurement of portlandite carbonation kinetics with supercritical CO2. **Chemical Geology**, v. 265, n. 1–2, p. 113–121, 15 jul. 2009.

ROOSZ, C. et al. Distribution of Water in Synthetic Calcium Silicate Hydrates. **Langmuir**, v. 32, n. 27, p. 6794–6805, 12 jul. 2016.

SCHULTE HOLTHAUSEN, R.; RAUPACH, M. Monitoring the internal swelling in cementitious mortars with single-sided 1H nuclear magnetic resonance. **Cement and Concrete Research**, v. 111, p. 138–146, 1 set. 2018.

SCRIVENER, K. L.; JUILLAND, P.; MONTEIRO, P. J. M. Advances in understanding hydration of Portland cement. **Cement and Concrete Research**, v. 78, p. 38–56, 2015.

SCRIVENER, K.; SNELLINGS, R.; LOTHENBACH, B. **A practical guide to microstructural analysis of cementitious materials**. [s.l: s.n.]. v. 1

TAJUELO RODRIGUEZ, E. et al. Thermal stability of C-S-H phases and applicability of Richardson and Groves' and Richardson C-(A)-S-H(I) models to synthetic C-S-H. **Cement and Concrete Research**, v. 93, p. 45–56, 1 mar. 2017.

ZAJAC, M. et al. CO2 mineralisation of Portland cement: Towards understanding the mechanisms of enforced carbonation. **Journal of CO2 Utilization**, v. 38, p. 398–415, 2020a.

ZAJAC, M. et al. Phase assemblage and microstructure of cement paste subjected to enforced, wet carbonation. **Cement and Concrete Research**, v. 130, n. January, p. 105990, 2020b.

ZAJAC, M. et al. Enforced carbonation of cementitious materials. **Cement and Concrete Research**, v. 174, 1 dez. 2023.